



HAL
open science

Evaluating surface and subsurface water storage variations at small time and space scales from relative gravity measurements in semiarid Niger

Julia Pfeffer, Cedric Champollion, Guillaume Favreau, Bernard Cappelaere, Jacques Hinderer, Marie Boucher, Yahaya Nazoumou, Monique Oi, Maxime Mouyen, Christopher Henri, et al.

► To cite this version:

Julia Pfeffer, Cedric Champollion, Guillaume Favreau, Bernard Cappelaere, Jacques Hinderer, et al.. Evaluating surface and subsurface water storage variations at small time and space scales from relative gravity measurements in semiarid Niger. *Water Resources Research*, 2013, 49 (6), pp.3276-3291. 10.1002/wrcr.20235 . hal-00857351

HAL Id: hal-00857351

<https://hal.science/hal-00857351>

Submitted on 21 Aug 2020

HAL is a multi-disciplinary open access archive for the deposit and dissemination of scientific research documents, whether they are published or not. The documents may come from teaching and research institutions in France or abroad, or from public or private research centers.

L'archive ouverte pluridisciplinaire **HAL**, est destinée au dépôt et à la diffusion de documents scientifiques de niveau recherche, publiés ou non, émanant des établissements d'enseignement et de recherche français ou étrangers, des laboratoires publics ou privés.

Evaluating surface and subsurface water storage variations at small time and space scales from relative gravity measurements in semiarid Niger

Julia Pfeffer,¹ Cédric Champollion,² Guillaume Favreau,³ Bernard Cappelaere,³ Jacques Hinderer,¹ Marie Boucher,^{3,4} Yahaya Nazoumou,⁵ Monique Oï,³ Maxime Mouyen,^{1,6} Christopher Henri,³ Nicolas Le Moigne,² Sébastien Deroussi,⁷ Jérôme Demarty,³ Nicolas Boulain,⁸ Nathalie Benarrosh,³ and Olivier Robert⁷

Received 18 May 2012; revised 21 March 2013; accepted 1 April 2013; published 10 June 2013.

[1] The acquisition of reliable data sets representative of hydrological regimes and their variations is a critical concern for water resource assessment. For the subsurface, traditional approaches based on probe measurements, core analysis, and well data can be laborious, expensive, and highly intrusive, while only yielding sparse data sets. For this study, an innovative field survey, merging relative microgravimetry, magnetic resonance soundings, and hydrological measurements, was conducted to evaluate both surface and subsurface water storage variations in a semiarid Sahelian area. The instrumental setup was implemented in the lower part of a typical hillslope feeding to a temporary pond. Weekly measurements were carried out using relative spring gravimeters during 3 months of the rainy season in 2009 over a $350 \times 500 \text{ m}^2$ network of 12 microgravity stations. Gravity variations of small to medium amplitude ($\leq 220 \text{ nm s}^{-2}$) were measured with accuracies better than 50 nm s^{-2} , revealing significant variations of the water storage at small time (from 1 week up to 3 months) and space (from a couple of meters up to a few hundred meters) scales. Consistent spatial organization of the water storage variations were detected, suggesting high infiltration at the outlet of a small gully. The comparison with hydrological measurements and magnetic resonance soundings involved that most of the microgravity variations came from the heterogeneity in the vadose zone. The results highlight the potential of time lapse microgravity surveys for detecting intraseasonal water storage variations and providing rich space-time data sets for process investigation or hydrological model calibration/evaluation.

Citation: Pfeffer, J., et al. (2013), Evaluating surface and subsurface water storage variations at small time and space scales from relative gravity measurements in semiarid Niger, *Water Resour. Res.*, 49, 3276–3291, doi:10.1002/wrcr.20235.

1. Introduction

[2] In Southwest Niger, as in many other parts of the semiarid Sahelian belt (Figure 1a), hydrological processes

display marked variability over a wide range of spatial and temporal scales, further impacted by climatic and land-use changes [e.g., Dolman *et al.*, 1997; Cappelaere *et al.*, 2009]. Driven by the West African monsoon, the wet season lasts only a few months and precipitation remains generally under 700 mm a^{-1} [e.g., Balme *et al.*, 2006]. Except for the Niger River, river flows are intermittent. Sporadic runoff is rapidly produced by intense convective storms and confined to small endorheic watersheds of a few square kilometers. The water accumulates in closed depressions creating temporary ponds, where it generally infiltrates toward the aquifer [Desconnets *et al.*, 1997]. Although most groundwater recharge occurs through these temporary ponds, percolation processes may also occur episodically at specific locations, such as sandy gullies [Massuel *et al.*, 2006; Descroix *et al.*, 2012] or banded vegetation areas [Bromley *et al.*, 1997; Galle *et al.*, 1999]. Infiltration remains otherwise limited to the near-soil surface, mainly due to high evapotranspiration demand [Cuenca *et al.*, 1997; Gaze *et al.*, 1997; Peugeot *et al.*, 1997; Esteves and Lapetite, 2003; Massuel *et al.*, 2006; Ramier *et al.*, 2009]. Strong interactions between groundwater resources and land surface conditions are well illustrated by the

Additional supporting information may be found in the online version of this article.

¹IPGS-EOST, CNRS/UdS, UMR 7516 Strasbourg, France.

²Géosciences Montpellier, UMR CNRS/UM2 5243, Université Montpellier 2, Montpellier, France.

³IRD, HydroSciences Montpellier, UM2 Montpellier, France.

⁴IRD, UJF-Grenoble 1, CNRS/G-INP, LTHE, Grenoble, France.

⁵Département de Géologie, Université Abdou Moumouni, Niamey, Niger.

⁶Institute of Earth Sciences, Academia Sinica, Taipei, Taiwan.

⁷Institut de Physique du Globe de Paris, Sorbonne Paris Cité, Université Paris Diderot UMR CNRS 7154, Paris, France.

⁸University of Technology Sydney, Plant Biology and Climate Change Cluster, Sydney, Australia.

Corresponding author: J. Pfeffer, IPGS-EOST, CNRS/UdS, UMR 7516, 5 rue René Descartes, FR-67084 Strasbourg CEDEX, France. (julia.pfeffer@unistra.fr)

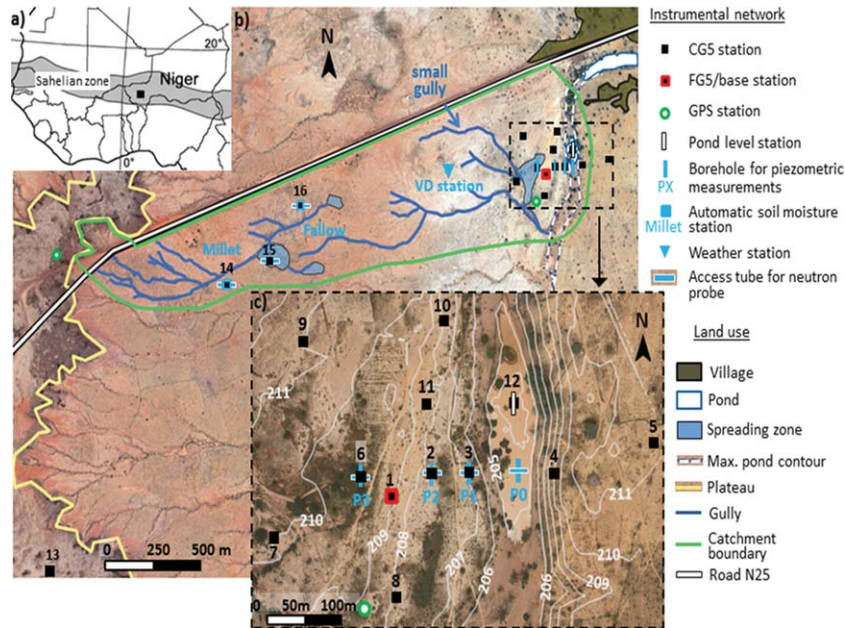


Figure 1. Description of the study area. (a) Location of the measurement site in Southwest Niger, West Africa. The black square represents the AMMA CATCH Niger observatory including Niamey and Wankama. Indicative limits of the Sahelian band are in gray, using the 200 and 700 mm mean annual isohyets for the period 1951–1989. Modified after Cappelaere *et al.* [2009]. (b) Instrumental setup. The terms CG5 and FG5 refer to the relative and absolute gravimeters, respectively. The main geomorphologic features of the Wankama catchment are outlined. The background photograph is a Spot image acquired on 23 October 2007 [Google Earth, 2010]. (c) Gravity network. Gray contour lines indicate the altitude (m) of the digital elevation model (DEM). The background aerial photograph is by J. L. Rajot, IRD, taken on 14 October 2008 (unpublished material); at this date, the pond water level was 1.15 m.

continuous rise in the groundwater table (~ 4 m) observed over the past 50 years [Favreau *et al.*, 2009], following widespread land cover changes [Leblanc *et al.*, 2008]. Land clearance led to more runoff production and hence to more focused groundwater recharge, in spite of severe drought conditions [Séguis *et al.*, 2004].

[3] Among the African Monsoon Multidisciplinary Analysis—Coupling the Tropical Atmosphere and the Hydrological Cycle (AMMA-CATCH) [Lebel *et al.*, 2009] observatories, dense instrumental networks were set up in the one-square degree Niamey area in Southwest Niger to investigate the relationship between climate, hydrology, vegetation, and land surface processes at various scales [Cappelaere *et al.*, 2009]. The data and knowledge collected pointed out the central role of land use and confirmed that, over a decadal time span, land cover changes had a greater impact on runoff production and groundwater recharge than the rainfall deficit [Séguis *et al.*, 2004; Boulain *et al.*, 2009; Massuel *et al.*, 2011]. However, finer process understanding and modeling is needed to explain the observed surface and subsurface fluxes and improve future water management scenarios [Cappelaere *et al.*, 2009]. In particular, intensive field work is required to (1) better represent the hydrological regime and critical aspects of its spatial variability, (2) refine the inventory of groundwater recharge points, and (3) evaluate the range and distribution of surface and subsurface properties [Cappelaere *et al.*, 2003; Massuel *et al.*, 2011]. Hydrological data could be

supplemented with high-resolution geophysical surveys to adequately resolve the system heterogeneity.

[4] Time-lapse gravity techniques are noninvasive and directly sensitive to the water mass variations without any petrophysical relationship. Gravity measurements integrate all the water masses, including surface water, soil moisture, and groundwater [e.g., Montgomery, 1971; Lambert and Beaumont, 1977; Bower and Courtier, 1998; Kroner, 2001; Creutzfeldt *et al.*, 2010a]. The volume sampled around the gravimeter ranges from several tens to hundreds cubic meters, typically to depths of a few meters to a few 10 m, depending on the spatial distribution of the water mass [e.g., Leirião *et al.*, 2009; Creutzfeldt *et al.*, 2008]. Gravity methods may be extremely useful to understand water storage dynamics or to constrain hydrological models [Hasan *et al.*, 2006, 2008; Krause *et al.*, 2009; Creutzfeldt *et al.*, 2010b, 2012; Naujoks *et al.*, 2010].

[5] Absolute free-fall gravimeters of FG5 type are able to detect hydrology-related variations in gravity, with accuracies in the range of $10\text{--}20\text{ nm s}^{-2}$ [Niebauer *et al.*, 1995], which can be compared to a variation by an equivalent water layer less than 5 cm thick. Absolute gravity measurements were recently performed in Southwest Niger and revealed a seasonal cycle linked to the West African monsoon of about 100 nm s^{-2} , which led to consistent evaluation of subsurface water storage variations [Pfeffer *et al.*, 2011]. However absolute gravity measurements can only investigate the water storage variations with limited spatial

and temporal resolutions, as measurements are very time consuming. Easier to transport and to operate, relative spring gravimeters are designed for intensive field work [e.g., *Jacob et al.*, 2010]. They allow spatial variations in gravity to be determined from a given station to a base station [e.g., *Christiansen et al.*, 2011a]. In classical relative gravity field surveys, the reference is chosen to be stable or must be monitored by an absolute gravimeter. Indeed, spring gravimeters are affected by a linear instrumental drift, which can be estimated by frequent measurements at the base station [e.g., *Naujoks et al.*, 2008; *Jacob et al.*, 2010]. Gravity differences can be achieved with an accuracy of 10–20 nm s⁻² in laboratory conditions with the Scintrex CG5 model [*Merlet et al.*, 2008]. In the field, the accuracy achieved with such sensors (usually 30–100 nm s⁻²) depends on the number and quality of the instruments used, the measurement procedure, and the exposure to external perturbations [e.g., *Bonvalot et al.*, 1998; *Gettings et al.*, 2008; *Naujoks et al.*, 2008; *Christiansen et al.*, 2011b].

[6] One of the main objectives of time-lapse microgravity surveys is to evaluate specific yield values from coincident monitoring of spatiotemporal variations in gravity and groundwater level over areas with contrasted hydrological behavior [e.g., *Pool and Eychaner*, 1995; *Pool*, 2008; *Gehman et al.*, 2009]. Seasonal variability in water storage has also been evidenced by microgravity surveys in various geological settings such as karstic systems [*Jacob et al.*, 2009, 2010], shallow groundwater mounds [*Chapman et al.*, 2008], and abandoned underground coal mines [*Davis et al.*, 2008]. Combined with continuous high-precision gravity records, microgravity measurements have demonstrated their potential for validating local hydrological models [*Naujoks et al.*, 2010]. Time-lapse microgravity data have also been used to calibrate groundwater models applied to an alluvial aquifer [*Christiansen et al.*, 2011a] as well as vadose zone models evaluated under forced infiltration conditions [*Christiansen et al.*, 2011c].

[7] Our survey aimed to investigate the variations in water storage over small time (from 1 week up to 3 months) and space (from a couple of meters up to a few hundred meters) scales in Sahelian Africa. The scale issue is a key point in this area as the processes controlling water storage dynamics (such as convective storms, Hortonian runoff or focused groundwater recharge) typically take place at scales from a couple of meters to a few hundred meters. For these reasons, a small (~350 × 500 m²) network of 12 gravity stations was set up around a temporary pond in Southwest Niger. Weekly gravity surveys were carried out for 3 months during the 2009 wet season as part of the first high-resolution gravity campaign in West Africa. Complementary and contemporary in situ observations were made in the framework of the AMMA-CATCH Niger observatory [*Cappelaere et al.*, 2009], including continuous rainfall, pond level, soil moisture, and groundwater table level measurements. In addition, magnetic resonance soundings (MRS) were employed to map heterogeneities in aquifer porosity. The data collected were analyzed to (1) test the ability of modern relative gravimeters to detect small amplitude signals under challenging field conditions, (2) quantify the variations in the water storage at small time and space scales, and (3) identify dynamic water storage com-

ponents. All of these objectives should help to improve our understanding and representation of the hydrological regime and determine critical features of its spatial and temporal variability. Such information would benefit further modeling studies, aiming to close the water budget and dynamics at various scales in the semiarid Sahelian environment.

2. Study Area

[8] The study area is part of a small (~2.5 km²) endorheic catchment, located in Southwest Niger, about 60 km east of the city of Niamey (Figure 1). The Wankama site has been chosen to host one AMMA-CATCH observatory [*Cappelaere et al.*, 2009] and part of the Gravity and Hydrology in Africa (GHYRAF) project [*Hinderer et al.*, 2009, 2011], because it is typical for the semiarid cultivated Sahelian environment regulated by the hydrological processes described earlier.

[9] The climate is tropical semiarid. Precipitation occurs in the form of intense convective storms during the wet season that lasts from June to October. The year 2009 was rather dry, with an annual rainfall of only 435 mm measured in Wankama compared with an average of 486 mm for the period 1990–2009. During the 3 months of the study period (7 July to 24 September 2009), daily air temperatures ranged from 20°C to 38°C, the precipitation reached 355 mm, and the reference evapotranspiration reached 390 mm (from Penman Monteith equation with local meteorological data).

[10] The Wankama catchment extends 3 km from west to east along a hillslope, reaching 260 m above mean sea level (AMSL) at the lateritic plateau and falling to 203 m AMSL at the pond (Figure 1b). The slopes on the west shore of the pond are gentle (≤2%), yet can reach 10% on the eastern side of the study area (Figure 1d). Detailed topography of the study area was achieved by a digital elevation model (DEM; Figure 1), derived from 3156 differential Global Positioning System (GPS) points collected over the catchment, including 1470 points in the 0.5 km² pond area [*Gendre et al.*, 2011]. The mean-square error between interpolated and measured elevations reached 0.03 m in the pond area (for a DEM with 5 m resolution) and 0.20 m for the whole catchment (for a DEM with a 20 m resolution). In addition, two permanent GPS stations (one on the plateau and one near the pond, see Figure 1b) were set up from 7 July to 24 September 2009 to evaluate the amplitude of the vertical displacements of the ground. Unfortunately, these GPS stations suffered from frequent power downs, increasing the level of noise in the data set (presented in Appendix 3 only, supporting information). The position of each gravimetric and hydrometeorological measurement point was evaluated with centimetric vertical accuracy from differential GPS measurements [*Gendre et al.*, 2011].

[11] The drainage network of the Wankama catchment includes several gullies conveying sporadic runoff toward the pond or sandy spreading zones (Figure 1b, background photograph from Google Earth [2010]). Part of the catchment surface also drains directly into the pond. The water accumulated in the pond then percolates toward the aquifer and/or is lost by evaporation. The Wankama catchment is

Table 1. Description of the Gravity Loops

Number of the Loop	Name of the Loop	Measurement Sequence
1	West-East	1–2–3–4–5–1
2	South	1–6–7–8–1
3	North	1–11–10–9–1
4	Pond	1–12–1
Appendix 2 (supporting information)	Plateau	1–13–14–15–16–1

covered with numerous rain-fed millet fields; ligneous vegetation is concentrated near ponds, or subsists as fallow [Séguis *et al.*, 2004]. The soils mainly consist of sand with a small fraction of fine particles (clay and silt) [Peugeot *et al.*, 2003]. They are classified as weakly leached tropical ferruginous soils [Commission Pédologique de Classification des sols, 1967] or Sandy Psammentic Haplustalf [Soil Survey Staff, 1975] and highly prone to erosion and crusting [Peugeot *et al.*, 2003].

[12] The underlying unconfined aquifer, about 30 m thick in average, belongs to the continental terminal (CT) formation [Lang *et al.*, 1990]. It is composed of loosely cemented sandstones of tertiary origin, which may contain a variable fraction of clays (e.g., 3%–41% in Massuel *et al.*, [2006]). The groundwater table is rather flat and lies around 190–200 m AMSL. Its depth, in average about 50 m, depends on topography: it varies from 10 m below the catchment pond to more than 60 m below the plateau. The hydraulic gradient is less than 0.1%, except near the pond where it can reach 1% during the seasonal aquifer recharge. The hydrogeological properties of the CT aquifer, recovered using MRS measurements and pumping tests, displayed high variability at both local (section 5) and regional scales with permeability and specific yield ranging between 1×10^{-5} to 3×10^{-4} m s⁻¹ and 1% to 9%, respectively, in Vouillamoz *et al.* [2008] and Boucher *et al.* [2009a, 2009b, 2012]. The aquiclude underlying the aquifer is a continuous impermeable gray-clayed layer, several dozen meters thick at an average depth of 80 m [Lang *et al.*, 1990].

3. Microgravity Measurements

3.1. Instrument Principle

[13] Two relative spring gravimeters of CG5 type manufactured by Scintrex (CG5) were used in this study. The device measures the difference in gravity from one site to another with a reading resolution of 10 nm s⁻² and a repeatability of less than 100 nm s⁻² [Scintrex Limited, 2009]. The gravity sensor is placed in a thermostatically stable vacuum chamber, operating with external temperature in the -40°C to +45°C range [Scintrex Limited, 2009]. The measurement relies on the extension of a vertical fused quartz spring, which supports a proof mass sensed by a capacitive displacement transducer. The external force required to bring back the proof mass to its reference position is proportional to the relative gravity value at the reading site and measured by an electrostatic feedback sensor [Scintrex Limited, 2009]. The natural creep of the

quartz spring induces a strong (~ 5000 nm s⁻² d⁻¹) instrumental drift, which can be assumed linear over a day in quiet environments [Bonvalot *et al.*, 1998] and evaluated by frequent reoccupation of the same base station [Merlet *et al.*, 2008]. During the measurement, the spring is aligned to the local vertical in the arc second range using a tripod especially designed for the CG5.

3.2. Experimental Strategy

[14] The survey aimed to detect hydrology-related gravity variations of small amplitude (a few 10 nm s⁻²) at small time and space scales. To reach these objectives, a trade-off must be made between accuracy, spatial, and temporal resolutions. Microgravity measurements were performed four times per week during 3 months (7 July to 24 September 2009) using two CG5s (serial number 167 and 424) over a small (350 × 500 m²) network of 12 stations. As much as possible, gravity stations were colocated with hydrological measurement sites and chosen to sample areas of contrasted hydrological behavior. Distance between the stations was kept within a few hundred meters to allow transportation on foot and frequent reoccupation of the base station. Both criteria contribute to reduced uncertainty on gravity measurements. Several occupations per station were required to compute reliable estimates of the relative gravity values and associated uncertainties for each survey. During the field campaign, each station was measured at least 20 times in each survey, leading to accuracies better than 50 nm s⁻². The simultaneous use of two gravimeters at each site during the same loop increased independence between the measurements and the robustness of microgravity estimates. The entire network was monitored in 4 to 5 days, leading to one gravity map per week over the study area.

3.3. Measurement Protocol

[15] Challenging field conditions (high and variable air temperature, no power network, and a bad access road) were met during the campaign. To achieve the accuracy required by hydrological studies (a few 10 nm s⁻²), the following protocol was implemented by each of the five operators performing the surveys:

[16] (1) The gravity network was measured in four loops (Table 1), which started and ended at the station 1 (called base station) used to evaluate the drift. The base station was always reoccupied in less than 4 h to preserve the drift linearity assumption. The base station was designed for absolute gravity monitoring (carried out on 14 July, 15 and 22 September 2009) and was made up of a cubic (1 m³) concrete pillar and protected from wind and rain by a traditional hut with a radius ~ 1.5 m. The absolute gravity measurements of 14 July 2009 (only presented in Appendix 1, supporting information) were perturbed by a violent storm (20 mm of precipitation in 30 min at the closest rain gauge).

[17] (2) The stations 2–11 were each equipped with a concrete pillar of smaller dimensions (0.3 m³) to support relative spring gravimeters. For each survey, the CG5s were installed exactly at the same azimuth and kept at constant height by a brass ring fixed to the CG5 tripod. In this

Table 2. Number of Loops Selected Per Survey

Survey	Time in 2009	Loop 1 « West-East »	Loop 2 « South »	Loop 3 « North »	Loop 4 « Pond »
1	7–10 Jul	4	4	4	0
2	13–16 Jul	3	3	4	3
3	20–23 Jul	3	4	3	1
4	28–30 Jul	3	4	4	2
5	3–7 Aug	3	4	4	0
6	11–13 Aug	4	4	3	0
7	17–20 Aug	3	3	3	0
8	24–27 Aug	4	3	4	2
9	2–4 Sep	4	4	3	2
10	7–9 Sep	3	4	4	1
11	14–17 Sep	4	4	3	3
12	21–24 Sep	4	3	4	3

way, errors related to variations in the height and position were avoided.

[18] (3) Four measurements were made at each station on two consecutive days with two different gravimeters. The comparison of these rapidly repeated surveys should return a gravity difference close to zero and help estimate the repeatability of the measurements. Indeed, if there is no heavy rain, no significant gravity variation should occur in a period of 2 days.

[19] (4) The CG5 were set up to record five measurements, averaging 60 s gravity series, performed at 6 Hz sampling rate. The sets evaluated in situ to be unreliable (conditions in (5)) were repeated one or two times. Taking into account the four repetitions performed in a week, each site was measured at least 20 times.

[20] (5) A selection process was applied to reduce the noise level of the microgravity data. The data were selected, if at least three consecutive measurements follow these criteria: they deviated by less than 50 nm s^{-2} from the mean gravity value measured at the station, their standard deviation was under 200 nm s^{-2} , their tilts were comprised in the $[-10; +10]$ arcsec range, the internal temperature varied by less than 0.2 mK , and the drift was less than 10 nm min^{-1} . The number of loops selected each week was listed in Table 2.

[21] (6) Vibrations caused by the wind were minimized by placing a dustbin upside down over the gravimeter, which was shaded from the sun by an umbrella. No measurements were made during the hottest part of the day (12:00–16:00, local time) to reduce heating effects.

[22] (7) The instruments were carefully transported from station to station by foot.

[23] (8) When the instrument was not measuring, it was left leveled in continuous monitoring. The power supply was provided by a system of solar panels and batteries.

[24] The protocol was slightly modified for the pond station (12 on Figure 1c). The station was equipped with a metal structure rising 2.53 m above the bottom of the pond and accessed by row boat. The measurements had to be taken in the absence of wind. They were set up to record 15 (instead of 5) 60 s gravity measurements sampled at 6 Hz. The CG5 “seismic filter” option, which removes low frequency measurements, was activated to reduce the noise caused by the vibrations of the structure. The loop lasted only 1 h, as it included only the measurement at the pond station. For four additional stations (13–16 in Figure 1b)

located higher on the hillslope and on the plateau, the instrument was transported by car, yielding much noisier measurements (only presented in Appendix 2, supporting information).

3.4. Data Processing

[25] To investigate the variations in water storage, relative gravity measurements had to be corrected for all the significant temporal effects within a loop ($<4 \text{ h}$). On larger time scale, the regional signals common to the stations of each loop cancel each other out. Solid Earth tides were removed using the WDD (Wahr Dehant Defraigne) parameters [Dehant *et al.*, 1999] in Tsoft software [Van Camp and Vauterin, 2005], ocean tide loading using the FES2004 (Finite Element Solution) ocean tide model [Lyard *et al.*, 2006], and the effects of atmospheric pressure using in situ measurements performed at the VD station (Figure 1), with an admittance of $-3 \text{ nm s}^{-2} \text{ h Pa}^{-1}$. The effects related to the polar motion were negligible ($<1 \text{ nm s}^{-2}$) within a few hours. Large-scale hydrological effects, shown to be significant on annual absolute gravity chronicle [Pfeffer *et al.*, 2011], could be neglected ($<1 \text{ nm s}^{-2}$) within a loop.

[26] Microgravity data were then corrected for linear drift by least square adjustment using the software package [Hwang *et al.*, 2002] MCGRAVI [Beilin, 2006] based on the inversion scheme of GRAVNET. The calibration correction factors of the CG5 167 and 424 were updated by the operator with an accuracy of 10^{-4} in June 2009 at the Aigoual calibration line in the Montpellier region, South of France. Each set of identical loop measured was processed separately for each survey, so that the reoccupation time between each individual surveys is minimized, and inaccuracies due to errors in the various applied corrections are reduced. Using the base station (x_0) as the reference, the relative gravity value g'_x (nm s^{-2}) at the station x can be expressed as

$$g'_x = g_x - g_{x_0}, \quad (1)$$

where g_x and g_{x_0} (nm s^{-2}) are the absolute gravity values at the stations x and x_0 at that same time.

3.5. Uncertainty Analysis

[27] Microgravimetric measurements are affected by many sources of uncertainty [e.g., Christiansen *et al.*, 2011b], resulting from instrument-specific errors (e.g., variations in internal temperature, sensitivity to microseismicity), measurement procedures (e.g., quality of the leveling, transport), and various corrections applied to the data (e.g., instrumental drift, calibration factor). The standard error, computed as the standard deviation of all the residual from least square adjustment inversion, provided an integral value of different sources of uncertainty for each station and each survey. As standard errors sometimes underestimate systematic errors, a threshold of 50 nm s^{-2} was added to the standard deviations measured before the inversion [e.g., Jacob *et al.*, 2010]. No significant correlation (correlation coefficient $R = 0.04$, p value < 0.001) was found between the internal temperature and the microgravity values. As the instruments were leveled with care and the sites were rather calm (low standard deviations during the measurements), a significant part of uncertainty may be due to

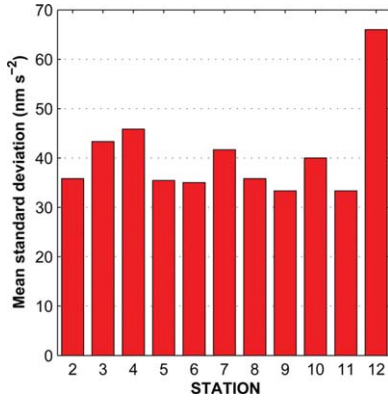


Figure 2. Mean uncertainties computed for the whole campaign with respect to the base station.

the imprecision of the drift adjustment (nonlinearity, jump due to the transportation). The standard errors reached on g^t values were averaged over the campaign period (7 July to 24 September 2009) and shown for all microgravity stations in Figure 2. The average standard errors were better than 50 nm s^{-2} for the stations 2–11. The uncertainty is generally under 50 nm s^{-2} for each station and each survey, because the inversion scheme takes into account several converging 60 s measurements following strict selection criteria. The error was higher (66 nm s^{-2} on average) at the pond site (12), because of the sensitivity of the metal structure to wind vibrations. The signal measured at this station exceeded 9.5 times the average error and was therefore considered significant.

3.6. Choice of the Relative Gravity Reference

[28] Microgravity values (g^t) are evaluated for a given station with respect to the base station (equation (1)). The spatial differences are mainly influenced by topography (from $-135,000$ to 7100 nm s^{-2} depending on the altitude of the considered station), but their temporal variations during the rainy season reflect the local variations in the water storage. Double gravity differences (Dg in nm s^{-2}) were introduced to estimate the time variable effects in gravity, and defined as

$$Dg_{x-x_0}^{t-t_0} = (g_x - g_{x_0})_t - (g_x - g_{x_0})_{t_0}, \quad (2)$$

where t is time (s) and t_0 initial time (s). The Dg values use for reference the time variations of the gravity value at the base station (g_{x_0}), which are unknown as no absolute measurements are available. Besides, the singular instrumental setup (a larger pillar and a hut) may have significantly reduced the microgravity signal measured at the base station, especially if induced by water storage variations located near the soil surface [Pfeffer, 2011, Figure 4.11, p. 66; Deville et al., 2013].

[29] To avoid the reference to a possibly singular station, a new variable denoted MDg (nm s^{-2}) was defined at station x and time t as the deviation of Dg from the mean Dg over the $n = 10$ downstream stations (2–11):

$$Dg_{x-x_0}^{t-t_0} - \overline{Dg_{x-x_0}^{t-t_0}} = (g_x - g_{x_0})_t - (g_x - g_{x_0})_{t_0} - \sum_{xi=1}^n \frac{(g_{xi} - g_{x_0})_t - (g_{xi} - g_{x_0})_{t_0}}{n}. \quad (3)$$

[30] The terms $(g_{x_0})_t$ and $(g_{x_0})_{t_0}$ related to the base station both cancel out, making the expression independent from the gravity value at the base station:

$$Dg_{x-x_0}^{t-t_0} - \overline{Dg_{x-x_0}^{t-t_0}} = (g_x)_t - (g_x)_{t_0} - \sum_{xi=1}^n \frac{(g_{xi})_t - (g_{xi})_{t_0}}{n}, \quad (4)$$

which can also be written as

$$MDg_x^{t-t_0} = \left(g_x - \sum_{i=1}^n \frac{g_{xi}}{n} \right)_t - \left(g_x - \sum_{i=1}^n \frac{g_{xi}}{n} \right)_{t_0}. \quad (5)$$

[31] In the final expression (equation (5)), MDg values do not use as reference the gravity value at the base station, but the mean gravity value over the $n = 10$ downstream stations. The interest of the new variable is to compare each station with the spatial average state of the system rather than with a particular station. The deviation from the mean gravity difference, MDg, provides a more legible expression of the spatial variability over the study area and was subsequently used to map variations in gravity in the vicinity of the pond.

3.7. Microgravity Maps

[32] Weekly gravity maps were computed after the first survey (t_0) as the deviation from the mean gravity difference (MDg) measured over the microgravity network ($n = 10$ stations), excluding the pond station (Figure 3). Contour lines were computed using a cubic interpolation and indicated each 20 nm s^{-2} . A positive MDg value indicates that, since the beginning of the gravity survey, the gravity increased more (or decreases less) at the considered station than the spatial average of the gravity network. Conversely, a negative MDg value indicates that the gravity increased less (or decreased more) than the spatial average of the gravity network. MDg values ranged between -120 and $+130 \text{ nm s}^{-2}$ during the 7 July to 24 September 2009 period. The gravity measurements revealed significant variations at small time and space scales, with a mean variance of the MDg values reaching 280 nm s^{-2} . Consistent spatial and temporal patterns emerged over this small ($\sim 350 \times 500 \text{ m}^2$) network. For example, the gravity signal was always positive at stations 6 and 2, whereas stations 5, 8, and 9 showed negative values in most of the surveys. Note that n , x_0 , and t_0 are fixed for the gravity campaign, so that the mean Dg depends only on t and is noted $\langle \Delta_t G \rangle$ on each map. The value of $\langle \Delta_t G \rangle$ increased during the campaign, meaning that gravity increased faster on average over the gravity network than at the base station. The largest increase in gravity ($630 \pm 145 \text{ nm s}^{-2}$) was recorded at the pond station (Figure 4).

4. Hydrometeorological Measurements

4.1. Instrumental Setup

[33] Rainfall was measured at 1 min intervals by a tipping-bucket rain gauge (Campbell Scientific RIMCO

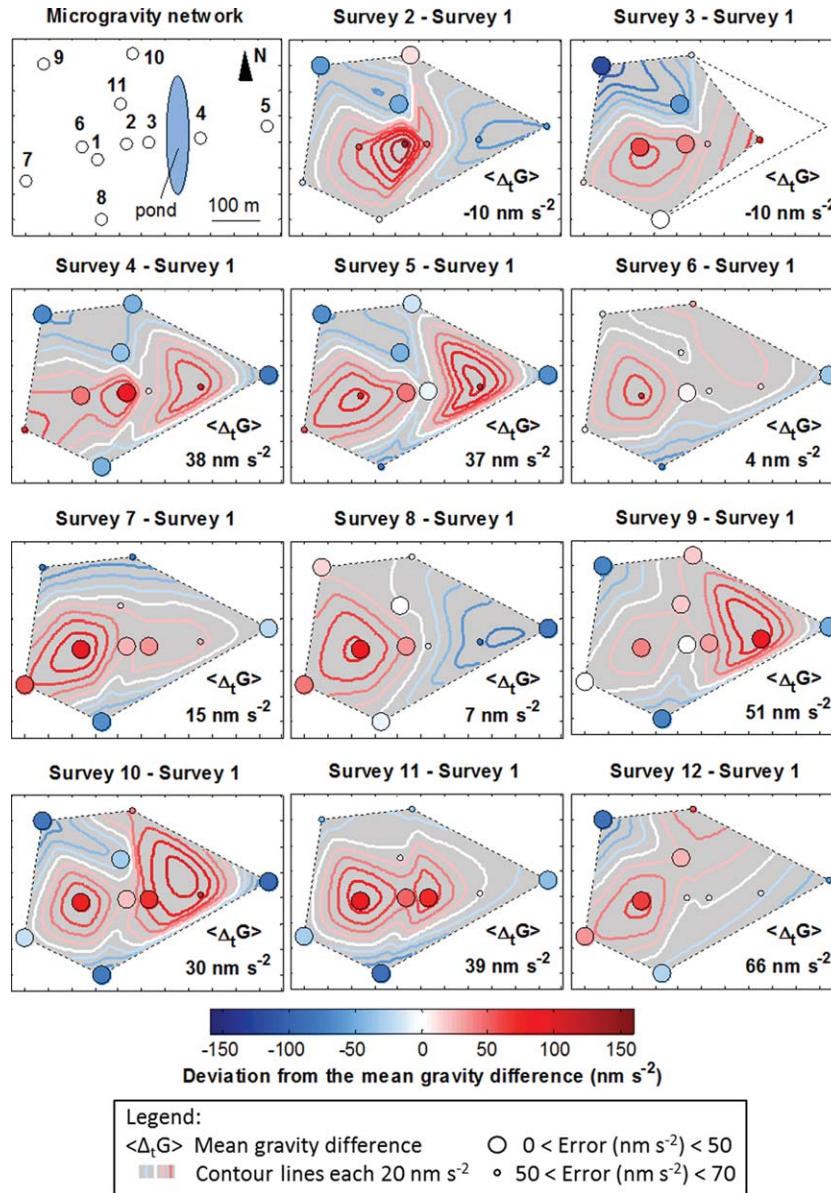


Figure 3. Weekly maps of the measured gravity signal. The relative gravity measurements are expressed as the deviation from the mean gravity difference (MDg; equation (5)). A positive MDg value indicates that, since the beginning of the survey, gravity increased more (or decreased less) at the considered stations than the spatial average of the gravity network. Conversely, a negative MDg value indicates that gravity increased less (or decreased more) than the spatial average of the gravity network. The dates of the beginning and end of each survey are listed in Table 2. Marks on x and y axes represent 50 m increments.

0.5 mm) located at the VD weather station (Figure 1). Rainfall data were not corrected for wetting losses or wind effect. Atmospheric pressure and temperature were measured at the VD station with a 1 min sampling interval. The pond level was measured at 5 min intervals, with a shaft encoder (OTT Thalimedes). The groundwater table level was evaluated at 20 min intervals with absolute pressure transducers (Eijkelkamp Micro-Diver) located in four boreholes at 0 (P0), 64 (P1), 110 (P2), and 210 (P3) m from the pond axis (Figure 1c). The atmospheric influence was corrected using in situ measurements carried out in Banizoum-

bou test site (~13 km away from Wankama) with a barometer (Eijkelkamp Baro-Diver). Direct measurements with a contact gauge (OTT KL010) were used to check the automatic piezometric data set. The soil volumetric water content was measured at 1 min intervals at two typical millet and fallow sites in the catchment by six reflectometers (Campbell Scientific CS616) buried at 0.1, 0.5, 1, 1.5, 2, and 2.5 m below the surface [Ramier *et al.*, 2009]. Access tubes for neutron probes were installed in the vicinity of the boreholes at the beginning of the 2009 rainy season. Weekly surveys were conducted with a neutron probe (ICT

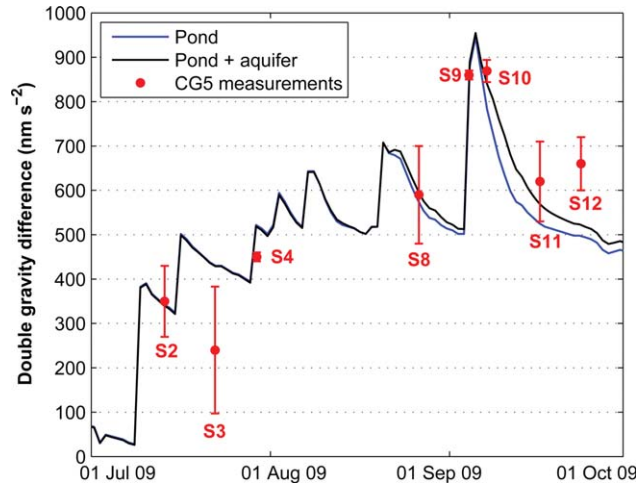


Figure 4. Comparison of the relative gravity signal measured at the pond station (red dots) with two models, taking into account the variation in the pond water level (blue line) or in the pond and groundwater levels table (black line). The aquifer model considers a heterogeneous distribution of porosities derived from MRS (Figure 6). The number X of the survey is indicated by SX beside each measurement point.

International CPN-503) down to a 10 m depth to estimate variations in the soil water content.

4.2. Hydrological Cycle During the 2009 Rainy Season

[34] Time variations in the water storage of the main reservoirs (pond, soil moisture, and groundwater) were continuously monitored during the 2009 rainy season (Figure 5). Just after the rainfall event on 7 July 2009, the pond started to fill up from dry past conditions (Figure 5b). The pond water level rose rapidly after each intense (≥ 20 mm) rainfall event and decreased during dry periods due to evaporation and infiltration. When the pond level reached its peak, the groundwater table rose by several meters in a few days (+2 m at P1 between 3 and 7 September; Figure 5d). In the meantime, a piezometric dome was formed below the pond, peaking at P1 with a hydraulic gradient of 0.5% between P3 and P1 (Figure 5a). The phenomenon was explained by rapid infiltration processes occurring below the pond, which increased when the water level reached the sandy layers at the shores of the pond [Descornets *et al.*, 1997]. On the long term, the groundwater table is rising in Wankama, gaining in average $+0.25 \text{ m a}^{-1}$ from the beginning of the piezometric measurements in 1993–2009. Measurements were made with neutron probes to monitor infiltration processes down to the groundwater table level in the vicinity of the pond (Figure 1). Unfortunately, weekly neutron probe measurements did not enable detection of significant variations in soil moisture at intraseasonal scale (only presented in Appendix 4, supporting information). The measurements made at the automatic soil moisture stations gave alternative information about the water storage processes in the first meters of soil under typical fallow and millet covers (Figure 5c). Major differences (up to 100 mm) were observed between the water stocks

($S_{3\text{m}}$ in mm) measured in the first 3 m of soil at the two sites and computed as

$$S_{3\text{m}} = 0.25 \cdot \theta_{0.1\text{m}} + 0.5 \cdot (\theta_{0.5\text{m}} + \theta_{1\text{m}} + \theta_{1.5\text{m}} + \theta_{2\text{m}}) + 0.75 \cdot \theta_{2.5\text{m}}, \quad (6)$$

where $\theta_{0.5\text{m}}$, $\theta_{1\text{m}}$, $\theta_{1.5\text{m}}$, $\theta_{2\text{m}}$, and $\theta_{2.5\text{m}}$ are the volume water content ($\text{m}^3 \text{ m}^{-3}$) measured at each probe. Such differences gave a first indication of the strong spatial variations in the water storage in the vadose zone.

5. Magnetic Resonance Soundings

5.1. Instrumental Setup

[35] A total of 17 MRS were performed over the study area in 2009–2010. The MRS method is directly sensitive to groundwater and allows the estimation of the vertical distribution of groundwater content [Legchenko *et al.*, 2004]. The measurement is based on the detection of the electromagnetic signal generated by the precession of the nuclei of the hydrogen atoms in groundwater molecules after electromagnetic excitation at a specific frequency (i.e., resonance frequency). For electronic reasons, the MRS signal cannot be recorded during an instrumental dead time, while the part of water which rapidly returns to equilibrium is not detected. The residual part of the groundwater content, measured by MRS, is assumed to be close to the effective porosity [Legtchenko *et al.*, 2004; Lubczynski and Roy, 2005].

[36] The NumisPlus equipment (Iris Instruments) was used with eight-shape loops made of two squares, whose sides measured 50 m. The radius investigated by MRS is of the same order of magnitude than the size of the loop (i.e., 100 m in our case). The depth of investigation was regulated down to ~ 100 m by the moment of the excitation pulse (in A ms). The MRS data were inverted in 1-D with Samovar software, assuming a homogeneous vertical distribution of the water content over the whole depth of the saturated aquifer. To decrease ambiguities in the interpretation, the aquifer geometry (groundwater table and aquiclude depths) was fixed using piezometric measurements at P0, P1, P3, and P3, time domain electromagnetic (TDEM) soundings, and available geological data. The methodology of the inversion, which takes into account the vertical distribution of electrical resistivity obtained by TDEM, was presented in detail in Boucher *et al.* [2009a].

5.2. MRS Map

[37] The inversion of MRS measurements enabled to determine the free water content of the saturated aquifer (θ_{MRS}), assumed to be a good estimate of the effective porosity [e.g., Vouillamoz *et al.*, 2008]. Previous studies carried out in the CT aquifer showed that θ_{MRS} values were systematically higher than Sy values estimated from pumping tests [Boucher *et al.*, 2009a, 2009b] and time-lapse absolute gravity surveys [Pfeffer *et al.*, 2011]. The difference would correspond to that portion of capillary water detected by MRS measurements, but that cannot be drained by gravity forces alone [Boucher *et al.*, 2009b; Pfeffer *et al.*, 2011].

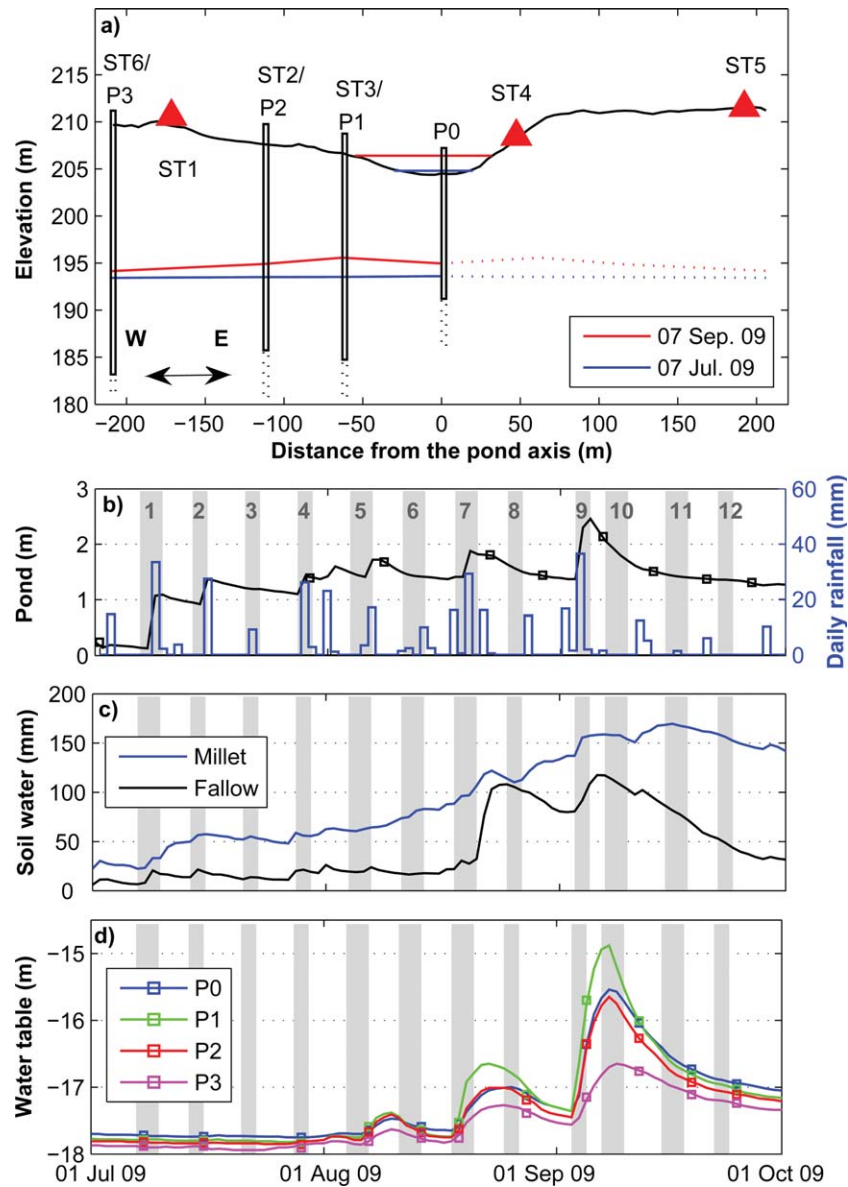


Figure 5. Hydrological parameters measured during the rainy season in 2009. (a) Cross section along the piezometric profile showing the pond and groundwater table levels during survey 1 (minimum groundwater table level) and survey 10 (maximum groundwater table level). The shape of the groundwater table is assumed to be linear between each of the four boreholes (solid lines) and symmetric with respect to the pond axis (dashed lines). The CG5 stations are indicated by red triangles denoted STX. Piezometers P1, P2, and P3 are collocated with CG5 stations 3, 2, and 6. (b) Temporal variations in the pond water level associated with the daily variations in rainfall measured at the VD gauge. The times of the microgravity surveys are indicated by numbered gray stripes. The squares represent visual readings of the water level. (c) Temporal variations in soil water stocks between 0 and 3 m at the fallow and millet sites. (d) Temporal variations in the groundwater table level recorded at the four piezometers. The groundwater table level corresponds to the depth of the groundwater table with respect to the altitude of the base station.

[38] The θ_{MRS} values resulting from the inversions of each sounding were attributed to the central position of the corresponding loop and then interpolated by kriging (Figure 6a). The mean value of θ_{MRS} is 12.5% over the study area. The θ_{MRS} values showed marked spatial variability (7%–18%), which may be explained by local geological

heterogeneities. The CT aquifer is indeed made of sandy to silty lenses of varying thickness and limited extent [Lang *et al.*, 1990]. The base station is located in a rather low porosity area ($\theta_{MRS}=10\%$), whereas station 10 is located near the area with the highest porosity ($\theta_{MRS}=18\%$).

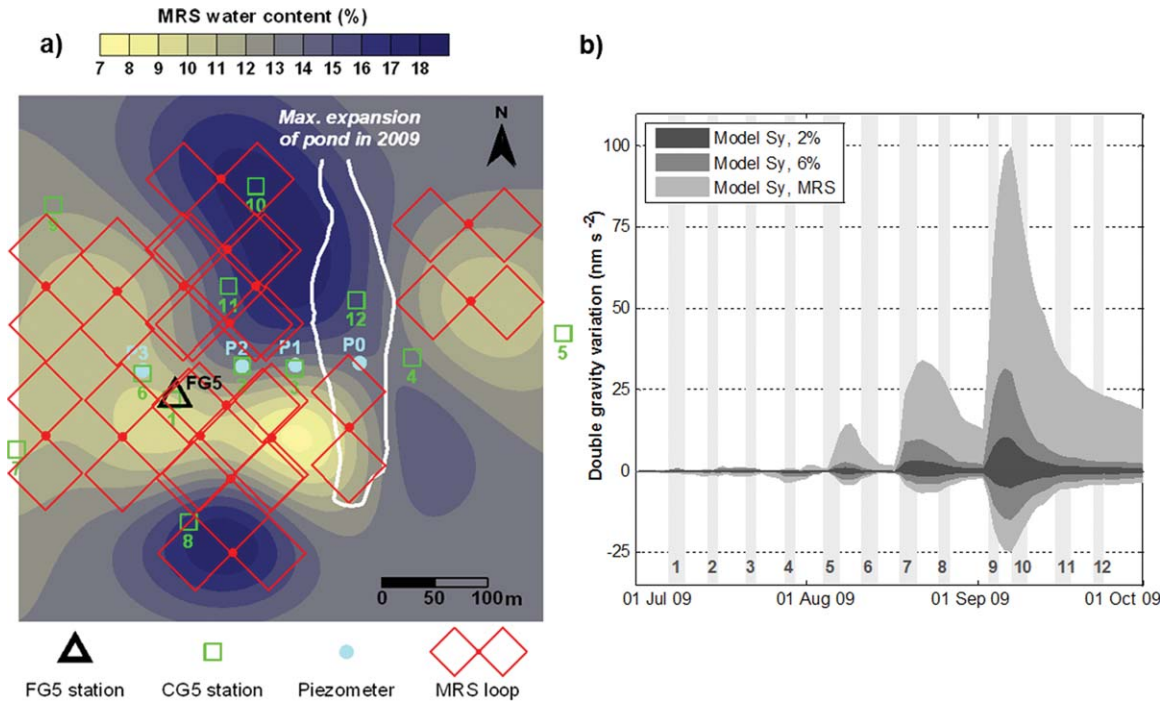


Figure 6. Modeled contributions of the aquifer to the relative gravity signal. (a) Distribution of the aquifer water content estimated by MRS. The maximal level reached by the pond in September 2009 is represented by the white line. (b) Range of variations in the modeled double gravity differences (D_g ; equation (2)) over the whole gravity network (including stations 2–12). The models Sy, 2% and Sy, 6% assume that Sy is constant and assigned to a value of 2% and 6% respectively, whereas in the model Sy, MRS assumes that Sy equals the MRS water content distribution mapped in Figure 6a. The times of the microgravity surveys are indicated by numbered gray stripes.

6. Water Storage Contributions to the Microgravity Signal

[39] The spatiotemporal variations in the gravity field, once corrected for large-scale geophysical effects, reflect variations in water storage in the pond, in the aquifer and in the vadose zone. As expected, the largest gravity variations were measured at the pond station, indicating that the maximum water storage (including surface, soil moisture, and groundwater reservoirs) occurred at the temporary pond. More insight about the internal hydrological behavior of the study area can be driven from the microgravity maps presented in Figure 3. Positive MDg values indicate that the water storage increased more (or decreases less) than the mean between the two surveys considered. Such variation in water storage may be transient (e.g., station 4, 7, or 10) or persistent (e.g., station 6, 2, or 3) throughout the rainy season. On the opposite, negative MDg values were detected near the stations 5, 8, and 11, suggesting that the water storage increased less (or decreased more) than average over the gravity network. The capacity to store more or less water in particular areas during a certain amount of time may be induced by structural heterogeneity (e.g., higher porosity) or dynamical processes (e.g., higher infiltration). When such trends are temporally persistent, a statistical relationship may be established between a specific location and the hydrological behaviour [e.g., Vachaud *et al.*, 1985]. For example, the station 6 (positive MDg

values) may be considered as a preferential water storage area, since more water than average is stored during the rainy season. The investigation of such spatial patterns is however limited by the strong intraseasonal variability evidenced by the microgravity measurements (Figure 3). Besides, the temporal stability concept is generally used to analyze the soil moisture variability [e.g., Brocca *et al.*, 2012], while microgravity measurements are sensitive to the water storage variations occurring from the soil surface down to the aquifer.

6.1. Contribution of the Pond

[40] The contribution of the pond was computed using the pond water level measurements and the 5 m resolution DEM produced for the pond area. The pond water volume was modeled at each measurement time by a configuration of right rectangular prisms, whose density equaled 10^3 kg m^{-3} . The gravitational attraction of each prism was computed using its exact analytical expression [e.g., Haaz, 1953; Nagy, 1966], and the contributions of each prism were summed. The resulting gravity variations were then summed at each microgravity station throughout the rainy season.

[41] A comparison between the modeled (in blue) and measured (in red) D_g values is presented for the pond station in Figure 4. Due to the difficulty of the measurement at the station, only eight microgravity values (equation (1))

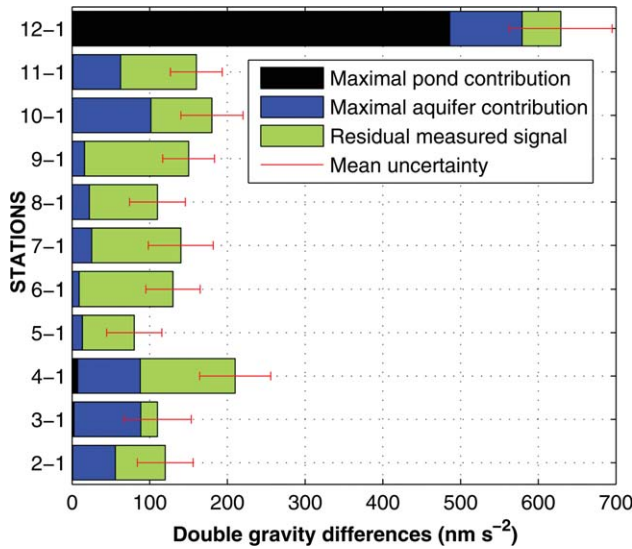


Figure 7. Maximal modeled amplitudes of the contributions of the pond (in black) and groundwater table (in blue) to the measured gravity signal (entire color bar). The residual measured signal (in green) is the difference between the maximal measured gravity signal (entire color bar) and the maximal contributions of the pond (in black) and aquifer using MRS water content distribution (in blue). The red error bars represent twice the uncertainty on double gravity differences (equation (2)), averaged over the whole campaign period.

were evaluated over the 12 surveys of the campaign. The maximum gravity signal ($630 \pm 145 \text{ nm s}^{-2}$) was measured between surveys 3 and 10, while the pond water level rose from 1.2 to 2.35 m (Figure 5b). The uncertainty on the measurements varied from 10 to 145 nm s^{-2} , depending on the number of loops selected for the inversion (Table 2) and on the noise incurred during the measurement (greatly influenced by wind). The model of the pond fluctuations explains a large proportion of the measured signal. The agreement was particularly fair for the surveys 9 and 10, which covered the highest stage of the pond. Some disparities were observed in the 100 nm s^{-2} range for surveys 3 and 12, corresponding to the same order of magnitude than the uncertainties on the microgravity values. Such differences could be explained by additional variations in the water storage occurring in the aquifer or in the vadose zone.

[42] The contribution of the pond to the gravity signal was found to be nonsignificant for the 10 other stations in the network. According to the pond model, the biggest rise in water level (+ 2.5 m) generated a maximum gravity variation of 8 nm s^{-2} at the station 4. The effect was negligible compared to the mean uncertainty (45 nm s^{-2}) reached at this station, and was even less at the other stations.

6.2. Contribution of the Aquifer

[43] The microgravity signal caused by the fluctuations in the groundwater table was computed using two different models, corresponding to minimum and maximum estimates of the aquifer contribution. The variations in the aquifer volume, calculated since 1 July 2009 (same initial time for all calculations) until 1 October 2009, were

described identically in both models, using a configuration of right rectangular prisms with a centimeter resolution in height. The groundwater table level was assumed to be linear between the piezometric measurements, symmetric with respect to the pond, constant in the north-south direction and flat beyond a radius of 500 m around the pond. The density of each prism was set as the density of water (10^3 kg m^{-3}) multiplied by the specific yield S_y (nondimensional number, defined as the fraction of groundwater that can be drained under gravity forces). The two models differ in their representation of the S_y values:

[44] (1) In the minimum aquifer model, the S_y value was assumed uniform and comprised in the range (2%–6%) determined by time-lapse absolute gravity surveys [Pfeffer *et al.*, 2011]. The contribution of the aquifer to Dg values was then found $<45 \text{ nm s}^{-2}$ when $S_y = 6\%$ and $<15 \text{ nm s}^{-2}$, when $S_y = 2\%$ (Figure 6b). The effect turned out to be small (and even negligible in the case of $S_y = 2\%$), because the only source of spatial heterogeneity was the hydraulic gradient raised during the formation of the piezometric dome (Figure 5a). The model was likely to underestimate the microgravity signal generated by the groundwater table fluctuations and could only be used as a lower limit for the aquifer contribution.

[45] (2) In the maximum aquifer model, the S_y values were assumed equal to the θ_{MRS} distribution (Figure 6a). The maximum amplitude (125 nm s^{-2}) of the simulated gravity signal was 2.8 times larger than with the previous model (Figure 6b). Indeed, when the porosity contrast between two stations was increased, the whole fluctuation zone contributed to the microgravity signal proportionally to the difference in S_y values. The real contribution of the aquifer is however expected to be less than this simulation, as θ_{MRS} values tend to overestimate S_y values [Boucher *et al.*, 2009a, 2009b; Pfeffer *et al.*, 2011]. The overestimation could be only partially alleviated by the geometrical model inaccuracies. Indeed, a variation of 0.15% on the hydraulic gradient (equivalent to an error of 30% on the maximum hydraulic gradient observed between P3 and P1) would have the same effect on the microgravity signal than a variation of 1% in average θ_{MRS} values. The ($S_y = \theta_{\text{MRS}}$) model can thus be considered as an upper limit of the aquifer contribution.

[46] The maximum contribution of the aquifer (using θ_{MRS}) was then compared to the maximum amplitude of the measured gravity signal (Figure 7). Both maxima may not occur at the same time, but their comparison gives an idea of the weight of the aquifer contribution in the gravity signal. At the pond station (12), most of the measured signal is explained by pond fluctuations. The contribution of the aquifer was low at this station, but helped to reproduce the gravity signal observed after the highest stage of the pond (survey 11, Figure 4). Except for stations 3 and 10, the maximum aquifer contribution was always less than half the maximum measured signal. However, the residual signal is expected to be larger than shown on Figure 7, because (1) the modeled aquifer contribution was overestimated, using θ_{MRS} as an estimate of S_y , and (2) the modeled aquifer contribution was significant only during surveys 9 and 10 (Figure 6b), while the measured microgravity signal displayed high spatiotemporal variations from the beginning to the end of the gravity campaign

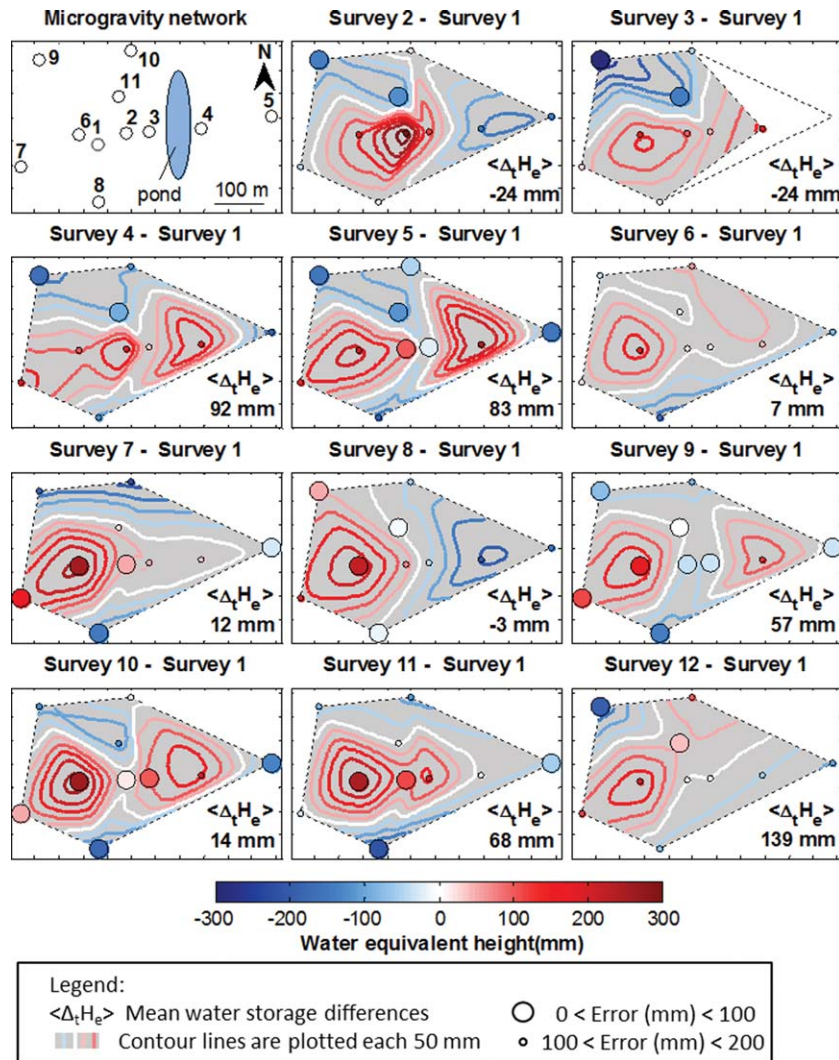


Figure 8. Weekly maps of the residual contribution of the vadose zone. The MDg values were corrected for the pond and aquifer effects and converted into water equivalent heights. Positive values indicate that the water storage in the vadose zone is above the mean of the whole gravity network, and conversely for negative values. The dates of the beginning and end of each survey are listed in Table 2. The marks on x and y axes represent 50 m increments.

(Figure 3). A large proportion of the gravity measurements could thus be explained neither by the pond nor by the aquifer contributions.

6.3. Contribution of the Vadose Zone

[47] The residual microgravity signal, evaluated after correction of the measurements for the pond and aquifer contributions, was attributed to the variations of the water content in the vadose zone. The effect of the aquifer was maximized using the upper limit ($S_y = \theta_{MRS}$) model, so that the residual gravity variations were the minimum expected. The residual microgravity values, either expressed with respect to gravity at the base station (D_g , equation (2)) or to the mean areal gravity (MDg, equation (5)), were converted into water equivalent heights (mm) using the Bouguer plate approximation:

$$\Delta g = 2\pi G\rho H, \tag{7}$$

where Δg ($m\ s^{-2}$) is the gravity increase due to the variation in water height H (m); G ($6.67 \times 10^{11}\ N\ m^2\ kg^{-2}$) the gravitational constant; and ρ ($10^3\ kg\ m^{-3}$) the density of water. According to equation (7), a gravity increase of $420\ nm\ s^{-2}$ corresponds to a 1 m increase in water height. The Bouguer-based conversion is only carried out to provide an order of magnitude of the water storage variations (in mm) that could explain the residual microgravity variations. An accurate inversion of the residual gravity signal would require three-dimensional modeling of the water storage variations in the vadose zone, including topographic effects [Creutzfeldt et al., 2008]. Neglecting the topography leads to a maximal error estimated at 10% of the vadose zone amplitude for the station near the pond.

[48] At the pond station (Figure 4), the residual D_g values were evaluated in the $100\text{--}150\ nm\ s^{-2}$ range (equivalent to 240–360 mm according to equation (7)), which can be compared to a change of 4%–6% in the water content

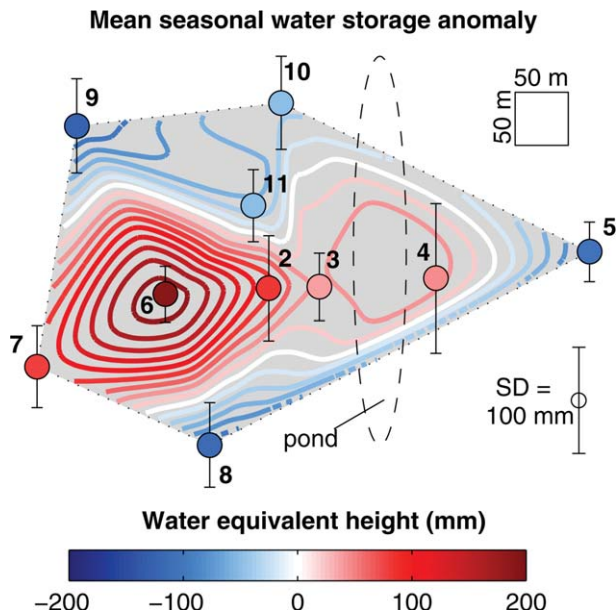


Figure 9. Mean seasonal residual contribution of the vadose zone. The MDg values corrected for the pond and aquifer effects are averaged over the whole gravity campaign (7 July to 24 September) and converted in water equivalent heights. The standard deviation (SD) values are computed at each station, to provide an indicator of the intraseasonal variability of the residual vadose zone signal. The errors on the mean seasonal water storage anomaly, ranging between 30 and 40 mm, are not displayed on this map. The number of each station is indicated besides each error bar. Contour lines are computed each 20 mm using a cubic interpolation.

distributed down to a depth of 6 m (the average infiltration depth determined by neutron probe measurements carried out on annual scale). The order of magnitude (4%–6%) is consistent with the S_y values estimated by gravimetry (2%–6%) and with θ_{MRS} values (7%–18%), which are known to overestimate S_y . Due to large uncertainties on microgravity measurements and the absence of reliable high-frequency soil moisture data, the interpretation of the residual signal at the pond station is limited.

[49] Over the remaining network (stations 2–11), time-lapse microgravity surveys enabled estimation of the dynamic variations in the water storage in the vadose zone, which ranged within ± 300 mm relative to the spatial mean (Figure 8). Such variations appear plausible in view of the soil moisture variability evidenced in the area [e.g., Cuenca *et al.*, 1997; Desconnets *et al.*, 1997] (Figure 5c) or derived from distributed hydrological modeling of the catchment [Cappelaere *et al.*, 2003; Boulain *et al.*, 2009]. The distribution of water in the vadose zone is indeed influenced by many sources of heterogeneity, including the topography, vegetation cover, state of the soil surface, and/or sharp spatial variability of rainfall due to its convective nature [e.g., Peugeot *et al.*, 2003]. Besides, very strong contrasts in upper soil hydraulic conductivity over the study area trigger water harvesting mechanisms at various scales,

whereby high infiltration areas collect large amounts of water from high runoff surfaces [Cappelaere *et al.*, 2009]. It results in a very large soil moisture variability, including at very local (<10 m) scales [e.g., Gaze *et al.*, 1997; Esteves and Lapetite, 2003].

[50] Preferential residual water storage areas were detected at stations 2, 6, and 7 (Figures 8 and 9). The maximum water storage anomaly reached +310 mm at station 6, with respect to the mean over the gravity network (Figure 8). The accumulation of water in the vadose zone could be explained by the release of the overland flow concentrated at the outlet of a small gully near station 6 (Figure 1b). The assumption is supported by frequent observations of rapidly drained pools and by a denser vegetation cover in the surroundings of the station 6 (Figure 1c), which suggests a greater availability of soil water at the outlet of the sandy gully. Additional information is provided by the mean water storage $\langle \Delta_r H_e \rangle$ values indicated on each map. It corresponds to the mean Dg value ($\langle \Delta_r G \rangle$) corrected for the pond and aquifer effects and converted into water equivalent heights. Positive $\langle \Delta_r H_e \rangle$ values (+40 mm on average during the gravity campaign) were observed, indicating that water storage was higher on average at the stations 2–11 than at the base station. The positive anomaly may be explained by soil crusting observed in the vicinity of the base station, dramatically reducing the infiltration capacity of degraded surfaces [Seguis *et al.*, 2004]. Human action can also significantly influence the water storage dynamics in the vadose zone, through farm work or trail tracking. Stations 15 and 5, located in millet fields, both appeared to store a relatively small amount of water in the vadose zone compared to the spatial average (Figure 8). However, land use does not determine point infiltration, as substantial variation can occur within a single field (e.g., from 0.3 to 3.4 times the rainfall observed by Gaze *et al.* [1997]). Photographic monitoring at the millet station (Figure 1b) in 2010 confirmed the large spatial variability of water distribution at the soil surface at a very small (~ 1 m) scale.

[51] The mean seasonal changes in water storage in the vadose zone were mapped over the gravity network in Figure 9 as a synthetic characterization of the vadose water storage. Obtained from the mean MDg values corrected for the pond and aquifer effects, they amount to the differences in water storage measured since the first survey with respect to the spatial mean over the gravity network, averaged over the full measurement campaign (7 July to 24 September 2009). The mean water storage anomalies ranged between -125 mm and $+190$ mm over the gravity network, revealing significant spatial variability in the vadose zone at local (~ 100 m) scale. Preferential water storage areas (i.e., positive values) were detected near stations 6, 7, and 2, whereas less water appeared to be stored on average at stations 5, 8, and 9 (values < -100 mm). The vadose zone signals evaluated at the microgravity stations display significant intraseasonal variability, as indicated by the high standard deviation reached during the gravity campaign (up to 140 mm at station 4). Detailed process-oriented studies would be necessary to discriminate the respective roles of infiltration, evapotranspiration, or geology as drivers of the variability of the vadose water storage.

7. Conclusions

[52] Time-lapse microgravity surveying is a noninvasive technique, directly sensitive to the variations in water storage occurring over several tens to hundreds of cubic meters from the soil surface to the aquifer. While relatively time consuming, the time-lapse microgravity technique could be particularly useful to capture small-scale hydrological signals that cannot be inferred from point measurements (e.g., soil moisture data or borehole) or catchment-scale data (e.g., discharge data). The field survey presented the first high-resolution microgravity measurements conducted in the semiarid Sahelian environment. Main results can be summarized as follows:

[53] (1) Time-lapse microgravity measurements were able to detect small-to-medium amplitude hydrology-related signals (in the $\pm 150 \text{ nm s}^{-2}$ range) in challenging field conditions. Transportation on foot, repeated measurements with two gravimeters, and a careful data quality check were necessary to achieve accuracies better than 50 nm s^{-2} .

[54] (2) Time-lapse microgravity measurements enabled quantification of significant heterogeneity in the water storage at small time (from 1 week up to 3 months) and space (from a couple of meters up to several hundred meters) scales.

[55] (3) Time-lapse microgravity measurements were greatly influenced by the variations in the water storage in the vadose zone. The maximum amplitude of those dynamic variations, after correction for the pond and aquifer effects, was evaluated in the order of $\pm 300 \text{ mm}$ with respect to the mean over the gravity network.

[56] Time-lapse microgravity surveys are a promising technique for water resource assessment in semiarid environments. Further field campaigns would usefully include supplemental absolute or superconducting gravity measurements, to enable estimation of temporal variations in the water storage at each station instead of only spatially relative signals. Neutron probe measurements would provide additional information on the vertical variation in the water content through the vadose zone, in and below the root zone down to the groundwater table. Indeed, if percolation processes have been evidenced under temporary ponds [Desconnets et al., 1997], large alluvial fans [Massuel et al., 2006] and main gully beds [Descroix et al., 2012], the interpretation of microgravity data suggested here that small gully outlets could also be concentrated infiltration sites and possibly contribute to aquifer recharge. If high and deep infiltration processes were confirmed by neutron probe measurements, stormwater concentrating areas could be identified at the outlet of small gullies (using aerial photograph or high resolution remote sensing imagery) and partially bridge the gap in water balance estimations in the area [Boucher et al., 2012; Massuel et al., 2011]. Further progress in the understanding of the subsurface hydrology dynamics could be achieved if the microgravity data were used in combination with distributed hydrological modeling of the catchment (ecohydrological model such as that of Boulain et al. [2009] and groundwater model as that of Massuel et al. [2011]), in order to better constrain both data interpretation and model trajectories and to ultimately improve quality of projections for this sensitive and quickly evolving environment. A gravity model could be associated

to the hydrological modeling in order to produce gravimetric outputs that could be directly compared with the microgravity measurements, and eventually to assimilate this type of data into hydrological models.

[57] **Acknowledgments.** This project is part of the Gravity and Hydrology in Africa (GHYRAF) project from 2008 to 2011 funded by the French *Agence Nationale de la Recherche* (ANR). Hydrological surveys were part of the regional AMMA-CATCH ecohydrological and meteorological observatory in West Africa (<http://www.amma-catch.org>), funded by the *Institut de Recherche pour le Développement* (IRD) and the *Institut National des Sciences de l'Univers* (INSU). The two Scintrex CG5 relative gravimeters were loaned by the Gravity Mobile facility (GMOB) of INSU. We thank the IRD in Niger for providing strong logistic and manpower support. We also like to acknowledge Jacques Beilin for his help with his software MCGRAVI. Finally, we thank the 20 students from the Department of Geology of the Faculty of Sciences at Abdou Moumouni University in Niamey (Niger) for their precious help and assistance in the field.

References

- Balme, M., T. Vischel, T. Lebel, C. Peugeot, and S. Galle (2006), Assessing the water balance in the Sahel: Impact of small scale rainfall variability on runoff—Part 1: Rainfall variability analysis, *J. Hydrol.*, *331*(1–2), 336–348, doi:10.1016/j.jhydrol.2006.05.020.
- Beilin, J. (2006), Apport de la gravimétrie absolue à la réalisation de la composante gravimétrique du Réseau Géodésique Français, Master thesis, Inst. Géogr. Natl., Paris, France.
- Bonvalot, S., M. Diament, and G. Gabalda (1998), Continuous gravity recording with Scintrex CG-3M meters: A promising tool for monitoring active zones, *Geophys. J. Int.*, *135*, 470–494.
- Boucher, M., G. Favreau, M. Descloitres, J. M. Vouillamoz, S. Massuel, Y. Nazoumou, B. Cappelaere, and A. Legchenko (2009a), Contribution of geophysical surveys to groundwater modelling of a porous aquifer in semiarid Niger: An overview, *C. R. Geosci.*, *341*, 800–809, doi:10.1016/j.crte.2009.07.008.
- Boucher, M., G. Favreau, J. M. Vouillamoz, Y. Nazoumou, and A. Legchenko (2009b), Estimating specific yield and transmissivity with magnetic resonance sounding in an unconfined sandstone aquifer (Niger), *Hydrogeol. J.*, *17*, 1805–1815, doi:10.1007/s10040-009-0447-x.
- Boucher, M., G. Favreau, Y. Nazoumou, B. Cappelaere, S. Massuel, and A. Legchenko (2012), Constraining groundwater modeling with magnetic resonance soundings, *Ground Water*, *50*(5), 775–784, doi:10.1111/j.1745-6584.2011.00891.x.
- Boulain, N., B. Cappelaere, L. Séguis, G. Favreau, and J. Gignoux (2009), Water balance and vegetation change in the Sahel: A case study at the watershed scale with an eco-hydrological model, *J. Arid. Environ.*, *73*, 1125–1135, doi:10.1016/j.jaridenv.2009.05.008.
- Bower, D. R., and N. Courtier (1998), Precipitation effects on gravity measurements at the Canadian Absolute Gravity Site, *Phys. Earth Planet. Int.*, *106*, 353–369, doi:10.1016/S0031-9201(97)00101-5.
- Bromley, J., J. Brouwer, A. P. Barker, S. R. Gaze, and C. Valentin (1997), The role of surface water redistribution in an area of patterned vegetation in a semiarid environment, south-west Niger, *J. Hydrol.*, *198*(1–4), 1–29, doi:10.1016/S0022-1694(96)03322-7.
- Cappelaere, B., B. E. Vieux, C. Peugeot, A. Maia, and L. Séguis (2003), Hydrologic process simulation of a semiarid, endoreic catchment in Sahelian West Niger, Africa. 2. Model calibration and uncertainty characterization, *J. Hydrol.* *279*, 244–261, doi:10.1016/S0022-1694(03)00182-3.
- Cappelaere, B., et al. (2009), The AMMA-CATCH experiment in the cultivated Sahelian area of south-west Niger—Investigating water cycle response to a fluctuating climate and changing environment, *J. Hydrol.*, *375*, 34–51, doi:10.1016/j.jhydrol.2009.06.021.
- Chapman, D. S., E. Sahm, and P. Gettings (2008), Monitoring aquifer recharge using repeated high-precision gravity measurements: A pilot study in South Weber, Utah, *Geophysics*, *73*(6), WA83–WA93, doi:10.1190/1.2992507.
- Christiansen, L., P. J. Binning, D. Rosbjerg, O. B. Andersen, and P. Bauer-Gottwein (2011a), Using time-lapse gravity for groundwater model calibration: An application to alluvial aquifer storage, *Water Resour. Res.*, *47*, W06503, doi:10.1029/2010WR009859.

- Christiansen, L., S. Lund, O. B. Andersen, P. J. Binning, D. Rosbjerg, and P. Bauer-Gottwein (2011b), Measuring gravity change caused by water storage variations: Performance assessment under controlled conditions, *J. Hydrol.*, 402(1–2), 60–70, doi:10.1016/j.jhydrol.2011.03.004.
- Christiansen, L., E. B. Haarder, A. B. Hansen, M. C. Looms, P. J. Binning, D. Rosbjerg, O. B. Andersen, and P. Bauer-Gottwein (2011c), Calibrating vadose zone models with time-lapse gravity data, *Vadose Zone J.*, 10(3), 1034–1044, doi:10.2136/vzj2010.0127.
- Commission Pédologique de Classification des sols (1967), *Classification des Sols*, p. 87, Ecole Natl. Supérieure d’Agronomie, Grignon, France.
- Creutzfeldt, B., A. Güntner, T. Klügel, and H. Wziontek (2008), Simulating the influence of water storage changes on the superconducting gravimeter of the Geodetic Observatory Wettzell, Germany, *Geophysics*, 73(6), WA95–WA104, doi:10.1190/1.2992508.
- Creutzfeldt, B., A. Güntner, H. Thoss, B. Merz, and H. Wziontek (2010a), Measuring the effect of local water storage changes on in-situ gravity observations: Case study of the Geodetic Observatory Wettzell, Germany, *Water Resour. Res.*, 46, W08531, doi:10.1029/2009WR008359.
- Creutzfeldt, B., A. Güntner, S. Vorogushyn, and B. Merz (2010b), The benefits of gravimeter observations for modelling water storage changes at the field scale, *Hydrol. Earth Syst. Sci.*, 14, 1715–1730, doi:10.5194/hess-14-1715-2010.
- Creutzfeldt, B., P. A. Ferré, P. A. Troch, B. Merz, H. Wziontek, and A. Güntner (2012), Total water storage dynamics in response to climate variability and extremes—Inference from long-term terrestrial gravity measurement, *J. Geophys. Res.*, 117, D08112, doi:10.1029/2011JD016472.
- Cuenca, R. H., et al. (1997), Soil measurements during HAPEX-Sahel intensive observation period, *J. Hydrol.*, 189(1–4), 224–266.
- Davis, K., Y. Li, and M. Batzle (2008), Time-lapse gravity monitoring: A systematic 4D approach with application to aquifer storage and recovery, *Geophysics*, 73(6), WA61–WA69, doi:10.1190/1.2987376.
- Dehant V., P. Defraigne, and J. M. Wahr (1999), Tides for a convective Earth, *J. Geophys. Res.*, 104, 1035–1058, doi:10.1029/1998JB900051.
- Desconnets, J. C., J. D. Taupin, T. Lebel, and C. Leduc (1997), Hydrology of the HAPEX-Sahel central super-site: Surface water drainage and aquifer recharge through the pool systems, *J. Hydrol.*, 189, 155–178.
- Descroix, L., et al (2012), Experimental evidence of deep infiltration under sandy flats and gullies in the Sahel, *J. Hydrol.*, 424–425, 1–15, doi:10.1016/j.jhydrol.2011.11.019.
- Deville, S., T. Jacob, J. Chéry, and C. Champollion (2013), On the impact of topography and building mask on time varying gravity due to local hydrology, *Geophys. J. Int.*, 192(1), 82–93.
- Dolman, A. J., J. H. C. Gash, J. P. Goutorbe, Y. Kerr, T. Lebel, S. D. Prince, and J. N. M. Stricker (1997), The role of the land surface in Sahelian climate: HAPEX-Sahel results and future research needs, *J. Hydrol.*, 189(1–4), 1067–1079.
- Esteves, M., and J.-M. Lapetite (2003), A multiscale approach of runoff generation in a Sahelian gully catchment: A case study in Niger, *Catena*, 50(2–4), 255–271, doi:10.1016/S0341-8162(02)00136-4.
- Favreau, G., B. Cappelaere, S. Massuel, M. Leblanc, M. Boucher, N. Boulain, and C. Leduc (2009), Land clearing, climate variability, and water resources increase in semiarid southwest Niger: A review, *Water Resour. Res.*, 45, W00A16, doi:10.1029/2007WR006785.
- Galle, S., M. Ehrmann, and C. Peugeot (1999), Water balance in a banded vegetation pattern—A case study of tiger bush in western Niger, *Catena*, 37(1–2), 197–216, doi:10.1016/S0341-8162(98)90060-1.
- Gaze, S. R., L. P. Simmonds, J. Brouwer, and J. Bouma (1997), Measurement of surface redistribution of rainfall and modeling its effect on water balance calculations for a millet field on sandy soil in Niger, *J. Hydrol.*, 188–189, 267–284, doi:10.1016/S0022-1694(96)03162-9.
- Gehman, C. L., D. L. Harry, W. E. Sanford, J. D. Stednick, and N. A. Beckman (2009), Estimating specific yield and storage change in an unconfined aquifer using temporal gravity surveys, *Water Resour. Res.*, 45, W00D21, doi:10.1029/2007WR006096.
- Genre, T., G. Ferhat, J. Hinderer, G. Favreau, B. Cappelaere, and E. Le Breton (2011), Évaluation de l’érosion du site de Wankama (Niger) par comparaison de différents MNT, *XYZ*, 129, 17–24.
- Gettings, P., D. S. Chapman, and R. Allis (2008), Techniques, analysis, and noise in a Salt Lake Valley 4D gravity experiment, *Geophysics*, 73(6), WA71–WA82, doi:10.1190/1.2996303.
- Google Earth (2010), Wankama, lat.: 13.560043° lon.: 2.648331, updated and composed by Google Earth on 15 Jan. 2010, www.earth.google.com. [accessed 31 Jan. 2011.]
- Haaz, I. B. (1953), Relations between the potential of the attraction of the mass contained in a finite rectangular prism and its first and second derivatives, *Geophys. Trans.*, 2, 57–66.
- Hasan, S., P. A. Troch, J. Boll, and C. Kroner (2006), Modeling the hydrological effect on local gravity at Moxa, Germany, *J. Hydrometeorol.*, 7, 346–354, doi:10.1175/JHM488.1.
- Hasan, S., P. A. Troch, P. W. Bogaart, and C. Kroner (2008), Evaluating catchment-scale hydrological modeling by means of terrestrial gravity observations, *Water Resour. Res.*, 44, doi:10.1029/2007WR006321.
- Hinderer, J., et al. (2009), The GHYRAF (Gravity and Hydrology in Africa) experiment: Description and first results, *J. Geodyn.*, 48, 172–181, doi:10.1016/j.jog.2009.09.014.
- Hinderer, J., et al (2011), Land water storage changes from ground and space geodesy: First results from the GHYRAF (Gravity and Hydrology in Africa) experiment, *Pure Appl. Geophys.*, doi:10.1007/s00024-011-0417-9.
- Hwang, C.W., Wang, C.G. and Lee, L.H. (2002), Adjustment of relative gravity measurements using weighted and datum-free constraints, *Computers and Geosciences*, 28, 1005–1015.
- Jacob, T., J. Chery, R. Bayer, N. Le Moigne, J. P. Boy, P. Vernant, and F. Boudin (2009), Time-lapse surface to depth gravity measurements on a karst system reveal the dominant role of the epikarst as a water storage entity, *Geophys. J. Int.*, 177, 347–360, doi:10.1111/j.1365-246X.2009.04118.x.
- Jacob, T., R. Bayer, J. Chery, and N. Le Moigne (2010), Time-lapse micro-gravity surveys reveal water storage heterogeneity of a karst aquifer, *J. Geophys. Res.*, 115, B06402, doi:10.1029/2009JB006616.
- Krause, P., M. Naujoks, M. Fink, and C. Kroner (2009), The impact of soil moisture changes on gravity residuals obtained with a superconducting gravimeter, *J. Hydrol.*, 373, 151–163, doi:10.1016/j.jhydrol.2009.04.019.
- Kroner, C. (2001), Hydrological effects on gravity data of the Geodynamic Observatory Moxa, *J. Geod. Soc. Jpn.* 47(1), 353–358.
- Lambert, A., and C. Beaumont (1977), Nano variations in gravity due to seasonal groundwater movements—Implications for gravitational detection of tectonic movements, *J. Geophys. Res.*, 82, 297–306.
- Lang, J., et al. (1990), The continental terminal in West Africa, *J. Afr. Earth Sci.*, 10, 79–99.
- Lebel, T., B. Cappelaere, S. Galle, N. Hanan, L. Kergoat, S. Levis, B. Vieux, L. Descroix, M. Gosset, E. Mougin, C. Peugeot, and L. Séguis, (2009), AMMA-CATCH studies in the Sahelian region of West-Africa: An overview, *J. Hydrol.*, 375, 3–13, doi:10.1016/j.jhydrol.2009.03.020.
- Leblanc, M. J., G. Favreau, S. Massuel, S. O. Tweed, M. Loireau, and B. Cappelaere (2008), Land clearance and hydrological change in the Sahel: SW Niger, *Global Planet. Change*, 61, 135–150, doi:10.1016/j.gloplacha.2007.08.011.
- Legchenko A., J. M. Baltassat, A. Bobachev, C. Martin, H. Robain, and J. M. Vouillamoz (2004), Magnetic resonance sounding applied to aquifer characterization, *Ground Water*, 42(3), 363–373, doi:10.1111/j.1745-6584.2004.tb02684.x.
- Leirião, S., X. He, L. Christiansen, O. B. Andersen, and P. Bauer-Gottwein (2009), Calculation of the temporal gravity variation from spatially variable water storage change in soils and aquifers, *J. Hydrol.*, 365, 302–309, doi:10.1016/j.jhydrol.2008.11.040.
- Lubczynski, M., and J. Roy (2005), MRS contribution to hydrogeological system parametrization, *Near Surf. Geophys.*, 3(3), 131–139, doi:10.3997/1873-0604.2005009.
- Lyard, F., F. Lefevre, T. Letellier, and O. Francis (2006), Modelling the global ocean tides: Modern insights from FES2004, *Ocean Dyn.*, 56, 394–415, doi:10.1007/s10236-006-0086-x.
- Massuel, S., G. Favreau, M. Descloîtres, Y. Le Troquer, Y. Albouy, and B. Cappelaere (2006), Deep infiltration through a sandy alluvial fan in semiarid Niger inferred from electrical conductivity survey, vadose zone chemistry and hydrological modelling, *Catena*, 67, 105–118, doi:10.1016/j.catena.2006.02.009.
- Massuel, S., B. Cappelaere, G. Favreau, C. Leduc, T. Lebel, and T. Vischel (2011), Integrated surface-groundwater modelling in the context of increasing water reserves of a Sahelian aquifer, *Hydrol. Sci. J.*, 56(7), 1242–1264, doi:10.1080/02626667.2011.609171.
- Merlet, S., A. Kopaev, M. Diamant, G. Geneves, A. Landragin, and F. P. Dos Santos (2008), Micro-gravity investigations for the LNE watt balance project, *Metrologia*, 45, 265–274, doi:10.1088/0026-1394/45/3/002.

- Montgomery, E. L. (1971), Determination of coefficient of storage by use of gravity measurements, PhD dissertation, Univ. of Ariz., Tucson.
- Nagy, D. (1966), The gravitational attraction of a right rectangular prism, *Geophysics* 31, 362–371.
- Naujoks, M., A. Weise, C. Kroner, and T. Jahr (2008), Detection of small hydrological variations in gravity by repeated observations with relative gravimeters, *J. Geod.*, 82, 543–553, doi:10.1007/s00190-007-0202-9.
- Naujoks, M., C. Kroner, A. Weise, T. Jahr, P. Krause, and S. Eisner (2010), Evaluating local hydrological modelling by temporal gravity observations and a gravimetric three-dimensional model, *Geophys. J. Int.*, 182, 233–249, doi:10.1111/j.1365-246X.2010.04615.x.
- Niebauer, T. M., G. S. Sasagawa, J. E. Faller, R. Hilt, and F. Klopping (1995), A new generation of absolute gravimeters, *Metrologia*, 32, 159–180, doi:10.1088/0026-1394/32/3/004.
- Peugeot, C., M. Esteves, S. Galle, J. L. Rajot, and J. P. Vandervaere (1997), Runoff generation processes: Results and analysis of field data collected at the East Central Supersite of the HAPEX-Sahel experiment, *J. Hydrol.*, 188–189, 179–202, doi:10.1016/S0022-1694(96)03159-9.
- Peugeot, C., B. Cappelaere, B. E. Vieux, L. Séguis, and A. Maia (2003), Hydrologic process simulation of a semiarid, endoreic catchment in Sahelian West Niger. 1. Model-aided data analysis and screening, *J. Hydrol.*, 279, 224–243, doi:10.1016/S0022-1694(03)00181-1.
- Pfeffer, J. (2011), Étude du cycle de l'eau en Afrique sahélienne: Approche multidisciplinaire et apport de la gravimétrie terrestre et spatiale, PhD dissertation, 206 pp., Univ. de Strasbourg, France.
- Pfeffer, J., M. Boucher, J. Hinderer, G. Favreau, J. P. Boy, C. de Linage, B. Cappelaere, B. Luck, M. Oi, and N. Le Moigne (2011), Local and global hydrological contributions to time-variable gravity in Southwest Niger, *Geophys. J. Int.*, 184, 661–672, doi:10.1111/j.1365-246X.2010.04894.x.
- Pool, D. R. (2008), The utility of gravity and water-level monitoring at alluvial aquifer wells in southern Arizona, *Geophysics*, 73, WA49–WA59, doi:10.1190/1.2980395.
- Pool, D. R., and J. H. Eychaner (1995), Measurements of aquifer-storage change and specific yield using gravity surveys, *Ground Water*, 33, 425–432, doi:10.1111/j.1745-6584.1995.tb00299.x.
- Ramier, D., et al. (2009), Towards an understanding of coupled physical and biological processes in the cultivated Sahel-1. Energy and water, *J. Hydrol.*, 375(1,2), 204–216, doi:10.1016/j.jhydrol.2008.12.002.
- Scintrex Limited (2009), *CG-5 Scintrex Autograv System Operation Manual*, rev. 4. [Available at <http://www.scintrexltd.com/gravity.html>].
- Séguis, L., B. Cappelaere, G. Milési, C. Peugeot, S. Massuel, and G. Favreau (2004), Simulated impacts of climate change and land-clearing on runoff from a small Sahelian catchment, *Hydrol. Processes*, 18, 3401–3413, doi:10.1002/hyp.1503.
- Soil Survey Staff (1975), *Soil Taxonomy: A Basic System on Soil Classification for Making and Interpreting Soil Surveys*, vol. 436, pp. 754, Soil Conserv. Serv., U.S. Dep. of Agric., Washington, D. C.
- Van Camp, M., and P. Vauterin (2005), Tsoft: Graphical and interactive software for the analysis of time series and Earth tides, *Comput. Geosci.*, 31, 631–640, doi:10.1016/j.cageo.2004.11.015.
- Vouillamoz, J. M., G. Favreau, S. Massuel, M. Boucher, Y. Nazoumou, and A. Legchenko (2008), Contribution of magnetic resonance sounding to aquifer characterization and recharge estimate in semiarid Niger, *J. Appl. Geophys.*, 64, 99–108, doi:10.1016/j.jappgeo.2007.12.006.